nature cell biology

Light-mediated activation reveals a key role for Rac in collective guidance of cell movement *in vivo*

Xiaobo Wang[1,3], Li He[1,3], Yi I. Wu[2], Klaus M. Hahn[2] & Denise J. Montell[1,4]

The small GTPase Rac induces actin polymerization, membrane ruffling and focal contact formation in cultured single cells[1] but can either repress or stimulate motility in epithelial cells depending on the conditions[2,3]. The role of Rac in collective epithelial cell movements *in vivo*, which are important for both morphogenesis and metastasis[4–7], is therefore difficult to predict. Recently, photoactivatable analogues of Rac (PA-Rac) have been developed, allowing rapid and reversible activation or inactivation of Rac using light[8]. In cultured single cells, light-activated Rac leads to focal membrane ruffling, protrusion and migration. Here we show that focal activation of Rac is also sufficient to polarize an entire group of cells *in vivo*, specifically the border cells of the *Drosophila* ovary. Moreover, activation or inactivation of Rac in one cell of the cluster caused a dramatic response in the other cells, suggesting that the cells sense direction as a group according to relative levels of Rac activity. Communication between cells of the cluster required Jun amino-terminal kinase (JNK) but not guidance receptor signalling. These studies further show that photoactivatable proteins are effective tools *in vivo*.

Border cells are a group of 6–8 cells that arise from the monolayer of ~650 epithelial follicle cells that surround 15 nurse cells and one oocyte in a structure called an egg chamber (Fig. 1a–c). Border cells migrate ~175 μm in between the nurse cells as an interconnected group of two distinct cell types: 4–8 migratory cells surround two central polar cells (Fig. 1d–i, k). Polar cells cannot migrate but secrete a cytokine that activates the Janus kinase/signal transducer and activator of transcription (JAK/STAT) pathway rendering the outer cells motile[9]. The outer cells carry the polar cells and lose the ability to move in the absence of continuous JAK/STAT activation[10]. Thus, each cell type requires the other. Border cells also require steroid hormone, receptor tyrosine kinase, Notch, and other signalling cascades[11–16]. Border cells therefore experience a rich and complex signalling environment, as do most cells *in vivo*.

The requirement for Rac in border cell migration was one of the earliest demonstrations of its role in cell motility *in vivo*[17]. Expression of either dominant-negative or constitutively active Rac impedes migration[13,17,18], suggesting that its activity must be spatially and/or temporally controlled. However, the precise function of Rac remains unclear.

To evaluate the effect of locally activating Rac in border cells, we generated transgenic flies expressing the photoactivatable form of Rac (PA-RacQ61L) tagged with the red fluorescent protein mCherry, under control of the Gal4/UAS system. When expressed in border cells using a Gal4 construct under the control of the *slow border cells* promoter (*slbo*-Gal4), the protein was distributed throughout the cells, in the cytoplasm and nuclei and at cell surfaces (Fig. 1g–i). In the absence of laser illumination, border cell migration was normal (Supplementary Information, Fig. S1; Movies S1 and S2).

Following exposure to repeated pulses of laser light, border cell migration could be redirected (Fig. 1l–t; Supplementary Information, Movie S3). In this example, border cells were migrating along the path designated by the solid arrow in Figure 1l, o and r and the leading cell extended a prominent forward-directed protrusion. The laser was applied to the cell next to the leading cell, which did not show any detectable protrusion at the time. Following illumination, the cluster retracted the original forward protrusion, changed direction and began moving to the side, a behaviour never observed in the wild type[19,20]. Light pulses were delivered once per minute owing to the reversibility of PA-Rac[8]. The border cells reached the side of the egg chamber after ~60 minutes (Fig. 1m, n and Supplementary Information, Movie S3). Although light pulses were continuously delivered, the cluster did not move further down the side of the egg chamber over the next 20 minutes (Fig. 1o–q), suggesting that there might be a barrier or repulsive cue in this region. When we shifted the site of illumination toward the centre of the egg chamber (Fig. 1r), the cells responded by moving in that direction (Fig. 1s, t; Supplementary Information, Movie S3). A single amino acid substitution in the LOV domain (C450M) renders the protein light-insensitive[8], and this construct could not redirect border cell migration even in the presence of light (Fig. 1u–w; Supplementary Information, Movie S4).

To determine whether Rac activity was required only in the lead cell, we co-expressed dominant-negative Rac (RacT17N) together with PA-RacQ61L in all border cells and photoactivated Rac in one cell. RacT17N alone strongly inhibits border cell motility[18] and photoactivation of Rac in

[1]Department of Biological Chemistry, Center for Cell Dynamics, Johns Hopkins School of Medicine, 855 North Wolfe Street, Baltimore, MD 21205 USA. [2]Department of Pharmacology, Lineberger Comprehensive Cancer Center, University of North Carolina, Chapel Hill, Chapel Hill, NC 27599, USA.
[3]These authors contributed equally.
[4]Correspondence and requests for materials should be addressed to D.J.M. (e-mail: dmontell@jhmi.edu).

Received 9 February 2010; accepted 8 April 2010; published online 16 May 2010; DOI: 10.1038/ncb2061

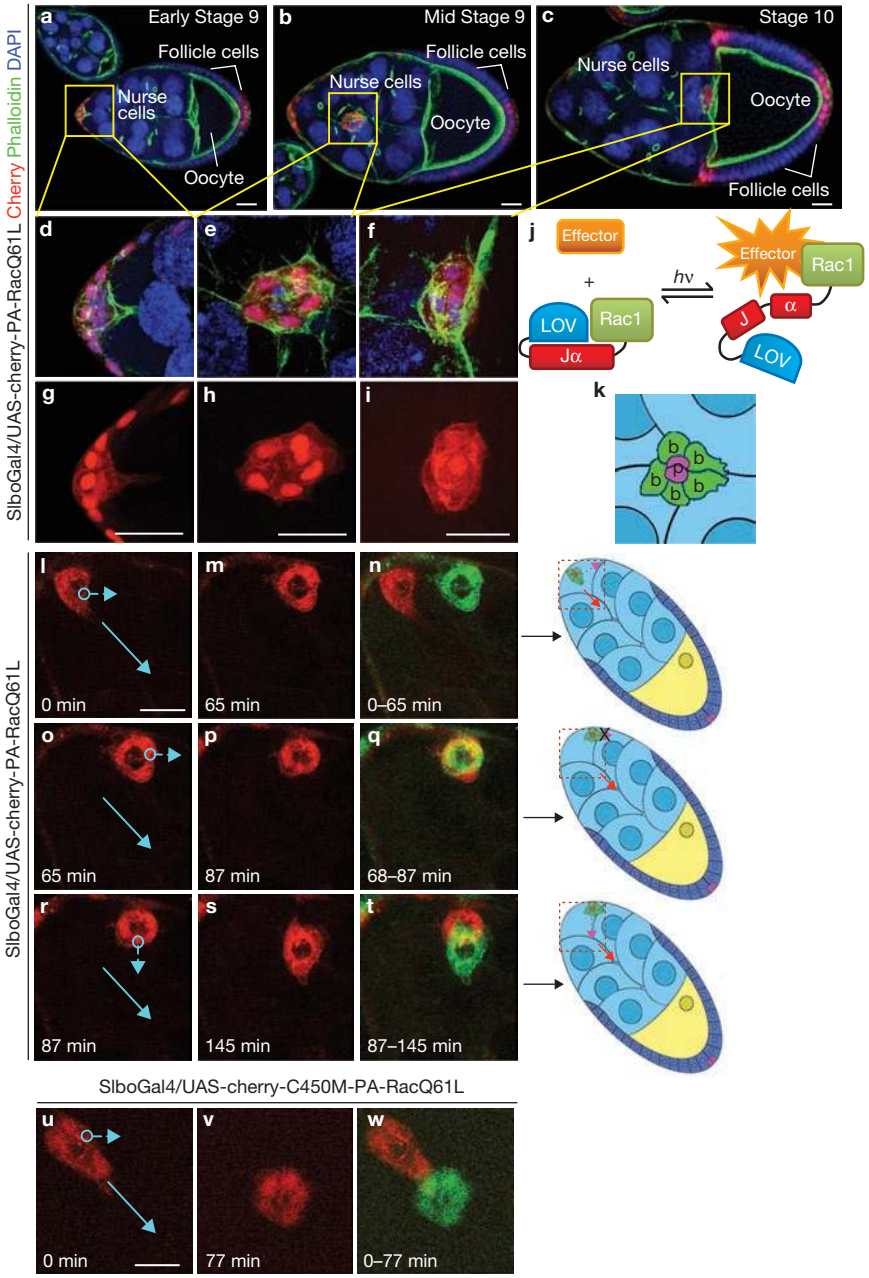

Figure 1 Local activation of PA-Rac1 redirects an entire border cell group. (**a**–**c**) Egg chambers labelled with 4,6-diamidino-2-phenylindole (DAPI, blue) to stain all nuclei, Alexa 488-phalloidin (green) to mark actin filaments, and mCherry (red) to show PA-RacQ61L. (**d**–**f**) Higher magnification views of border cells from each stage. (**g**–**i**) PA-RacQ61L expression only. (**j**) Schematic diagram showing the mechanism of PA-Rac activation by light (*hν*). (**k**) Schematic of a border cell cluster composed of two non-migratory polar cells (purple, p), which do not express *slbo*-Gal4 and are therefore unlabelled in all subsequent images. Polar cells are surrounded by 4–6 migratory border cells (green, b). (**l**–**t**) Selected still images from a time-lapse movie of the response of border cells to photoactivation of PA-RacQ61L. (**l**–**n**) Photoactivation diverts border cells to the edge of the egg chamber. (**o**–**q**) Continued photoactivation in same direction did not move them further along the edge. (**r**–**t**) Photoactivation of the same cluster in a different position drove movement towards the egg chamber centre. In **n**, **q** and **t** the starting position of the cluster is shown in red and the final position in green. Schematics at right show the position of the treated cluster within the egg chamber. Red boxes indicate the regions shown in the micrographs; red arrow indicates the normal direction of migration; pink arrow shows the direction the cells move if they respond to the light. (**u**–**w**) Phototreatment of light insensitive control C450M-PA-Rac1Q61L. In **l**, **n**, **q** and **u**, solid arrows indicate the normal direction of migration; circles indicate where the laser light was applied. Dashed arrows indicate the direction the cells move if they respond to the light. Scale bars, 20 μm.

the front cell failed to promote forward movement of the cluster in this background (Supplementary Information, Fig. S1g–i). However, activating Rac in approximately half of the cells in the cluster caused them to move forward, albeit very slowly (Supplementary Information, Fig. S1j–m. These results suggest that each cell requires some Rac activity for motility, and each cell contributes to the migration speed of the cluster, but the highest level of Rac activation determines the direction of movement.

We then tested whether PA-RacQ61L was sufficient to cause border cells to move in a direction opposite to their normal movement (Fig. 2). Border cells expressing PA-RacQ61L were first driven in the normal

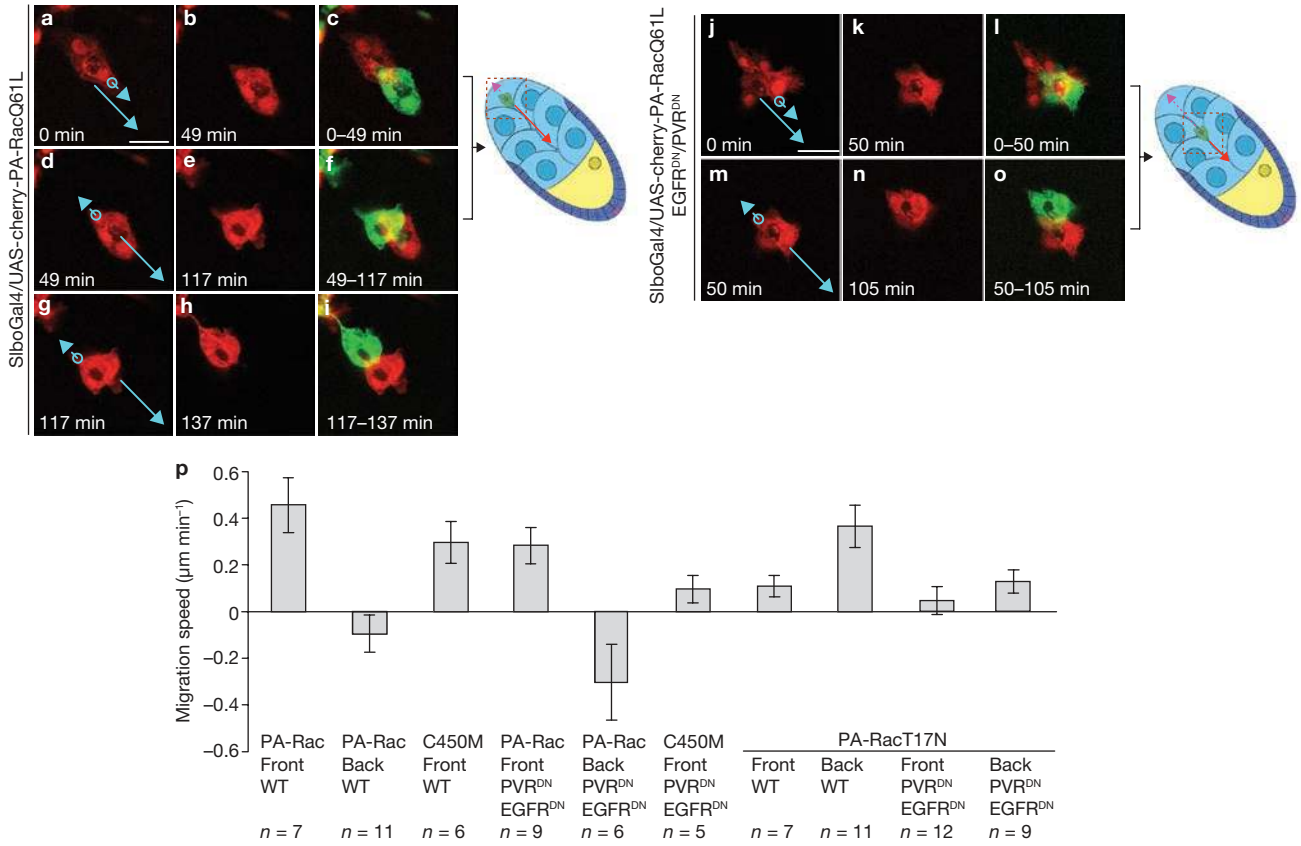

Figure 2 Forward or backward movement in response to photoactivatable Rac. (**a**–**i**) In an otherwise wild-type background, PA-RacQ61L can promote forward (**a**–**c**) or backward (**d**–**i**) movement. (**j**–**l**) Forward and (**m**–**o**) backward migration of border cells expressing PVR^{DN}, $EGFR^{DN}$ and PA-RacQ61L. The schematics at the right show the position of the cluster within the egg chamber. Scale bars, 20 μm. In **c**, **f**, **i**, **l** and **o**, red represents the starting position and green shows the ending position over the indicated time period. (**p**) Average migration speeds for clusters expressing the indicated proteins in response to illumination of the front or the back of the cluster. PA-Rac refers to PA-RacQ61L; C450M is the light-insensitive control. Values represent the average of the indicated number (*n*) of experiments and error bars show the s.d.

direction, and prominent lamellipodia-like protrusion was evident at the site of illumination (Supplementary Information, Movie S5). Then we illuminated the rear. Front protrusion ceased rapidly (Supplementary Information, Movie S5) but rearward movement was initially very slow. After a variable delay, clusters moved backwards (Fig. 2d–i), sometimes reconnecting with a follicle cell within the epithelium (Supplementary Information, Movie S5). In contrast, the light-insensitive control protein did not reverse the migration direction (Supplementary Information, Movie S6). On average, the PA-Rac-induced forward migration speed exceeded the reverse migration speed by 4.5-fold (Fig. 2p, PA-Rac Front versus PA-Rac Back), suggesting an influence of endogenous directional signalling on the behaviour induced by PA-Rac.

To explore the interaction between endogenous signals and PA-Rac, we compared the responses of wild-type cells to those of cells with reduced guidance receptor activity. The platelet-derived growth factor/vascular endothelial growth factor receptor (PVR) and the epidermal growth factor receptor (EGFR) are receptor tyrosine kinases that function redundantly to guide migrating border cells[13–15]. Border cells expressing dominant-negative forms of both guidance receptors, PVR^{DN} and $EGFR^{DN}$, extend protrusions in all directions and make little forward progress[20]. PA-Rac rescued both the morphological defect and directional movement in this genotype (Fig. 2j–l), consistent with the idea that Rac normally functions downstream of the receptors to determine the direction of movement. When clusters were illuminated at the front, the cells moved forward (Fig. 2j–l). When the same clusters were illuminated at the back, rearward movement resulted (Fig. 2m–o). In contrast to the responses of wild-type clusters, average forward and reverse migration speeds were indistinguishable in border cells expressing PVR^{DN} and $EGFR^{DN}$ (Fig. 2p), supporting the idea of competition between endogenous guidance receptor signalling and PA-Rac-induced directionality.

After stimulating rearward protrusion, we stopped illuminating and observed the recovery (Supplementary Information, Fig. S2). Both wild-type and PVR^{DN}- and $EGFR^{DN}$-expressing clusters rapidly protruded in response to rear illumination and retracted the rearward protrusion following cessation of the light. However, wild-type cells protruded less and retracted more (Supplementary Information, Fig. S2q). Over longer time courses, wild-type cells typically stalled after cessation of rear illumination but eventually recovered movement in the normal forward direction (Supplementary Information, Fig. S3a–m). In contrast, PVR^{DN}- and $EGFR^{DN}$-expressing clusters failed to recover forward movement (Supplementary Information, Fig. S3n–y). These results also suggest that endogenous PVR and EGFR signals compete with PA-RacQ61L-induced polarization.

The inability of PA-RacQ61L to cause border cells to move down the side of the egg chamber led us to probe the microenvironment further. Within about the anterior third of their normal travel path, focal Rac

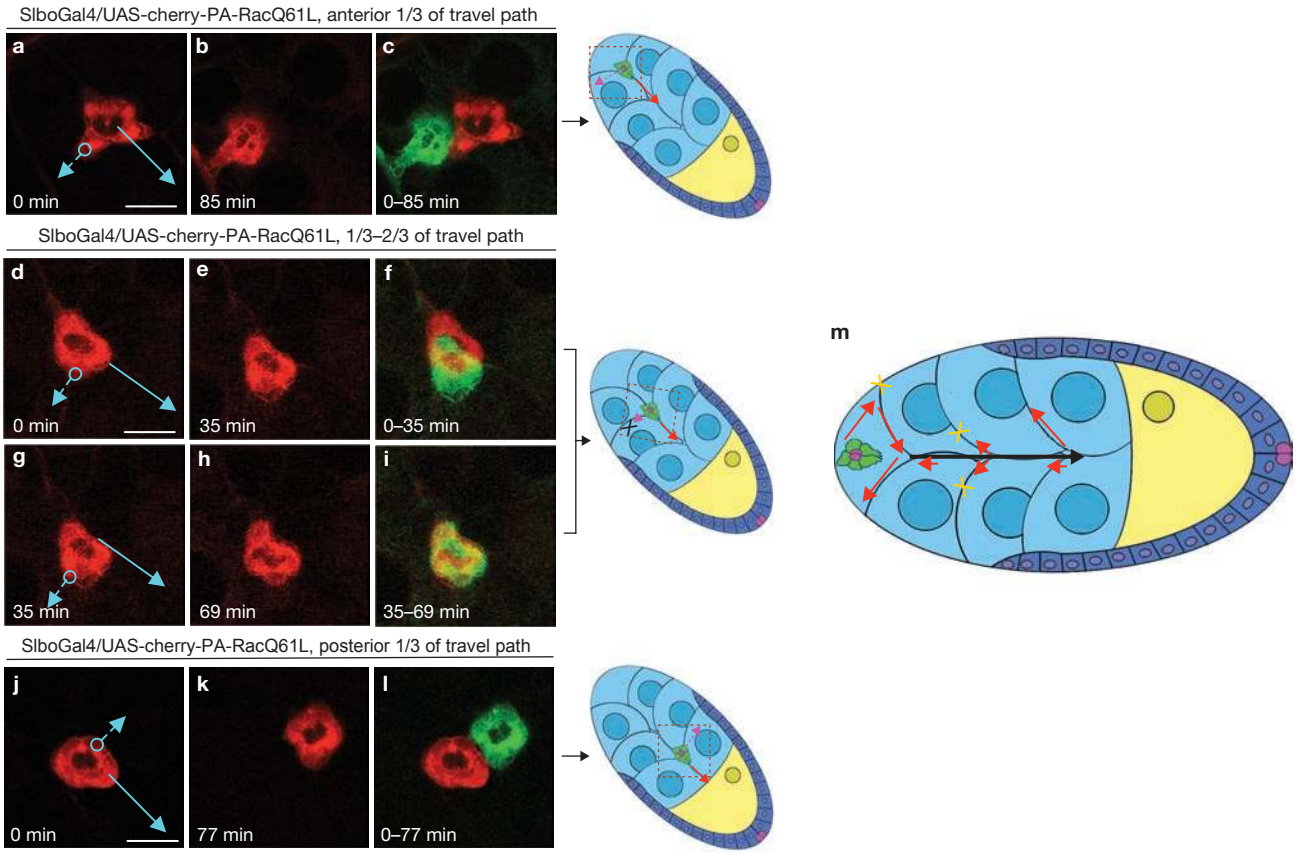

Figure 3 Responsiveness of border cells to PA-RacQ61L depends on their location within the egg chamber. (**a**–**c**) Within the anterior third of the egg chamber, photoactivation diverts border cells. (**d**–**i**) In the middle third, photoactivation has little effect. (**j**–**l**) In the posterior third, photoactivation again drives border cells toward the side. Scale bars, 20 μm. Schematics show border cell position within the egg chamber. In **c**, **f**, **i** and **l**, red indicates the starting position and green shows the ending position. (**m**) Summary of experiments. The lengths of the arrows indicate the average distance migrated in the indicated direction in response to PA-RacQ61L, for border cells starting at the base of the arrow. The black arrow indicates the normal migration direction. Yellow Xs indicate positions beyond which border cells did not move. Each arrow summarizes at least five experiments.

activation could steer border cells from the centre path all the way to the follicle cells, or along the perimeter of the egg chamber (Fig. 3a–c and m). However, if we treated cells after they reached the centre of the egg chamber, they could not be redirected to the follicle cell layer (Fig. 3d–i and m), although PA-RacQ61L could still move them forwards or backwards. Within the posterior third of their normal path, the cells could again be directed off their normal course, in between the nurse cells (Fig. 3j–l and m). A summary of the responses to PA-RacQ61L is shown in Fig. 3m. Thus, there are regions in the egg chamber that actively repel the border cells or lack important structural or chemical substrates for migration, suggesting that there is additional guidance information besides the ligands for PVR and EGFR.

PA-RacQ61L was also insufficient to cause border cells to migrate earlier than normal, possibly because high levels of JAK/STAT signalling, which are required for the border cells to initiate movement, are not achieved at earlier time points[21,22]. Consistent with this, PA-RacQ61L did not cause protrusion or migration in border cells expressing a dominant-negative form of the receptor Domeless, which is required for STAT activation (Supplementary Information, Fig. S4a–f). A key downstream target of STAT is the transcription factor SLBO[23], and *slbo* mutant border cells cannot extend protrusions. However, PA-RacQ61L could not rescue protrusion or migration in *slbo* mutants (Supplementary Information, Fig. S4 g–l). PA-RacQ61L also failed to rescue guidance receptor deficiency after stage 10 (not shown). Together, these findings demonstrate that PA-RacQ61L reveals temporal as well as spatial constraints on migrating cells.

To evaluate the effects of locally inhibiting Rac, we generated transgenic flies expressing PA dominant-negative Rac (UAS-PA-RacT17N). Illuminating the leading border cell arrested migration and, strikingly, led to protrusion at the cluster rear (Supplementary Information, Fig. S5a–j; Supplementary Information, Movie S7). In contrast, illumination of the rear of the cluster enhanced forward protrusion (Supplementary Information, Fig. S5k–m) and migration (Fig. 2p). The magnitude of the effect was smaller in PVR^{DN}- and $EGFR^{DN}$-expressing cells (Supplementary Information, Fig. S5n–p; Fig. 2p).

The non-autonomous effects of PA-RacQ61L and PA-RacT17N were striking, so we examined the morphological consequences at higher magnification. Specifically, activation of Rac in one cell of either a wild-type cluster (Fig. 4a–c) or a cluster expressing PVR^{DN} and $EGFR^{DN}$ (Fig. 4d–f) resulted in retraction of protrusions by the other cells and movement of the cluster in the direction of the light. This was true whether the illumination was provided at the front of the cluster (not shown) or at the back. PA-RacT17N had precisely the opposite effect in a polarized wild-type cluster (Fig. 4j–l). Focal inhibition of Rac in the protruding lead cell caused a loss of polarization and random protrusion of all the cells in the cluster (Fig. 4l).

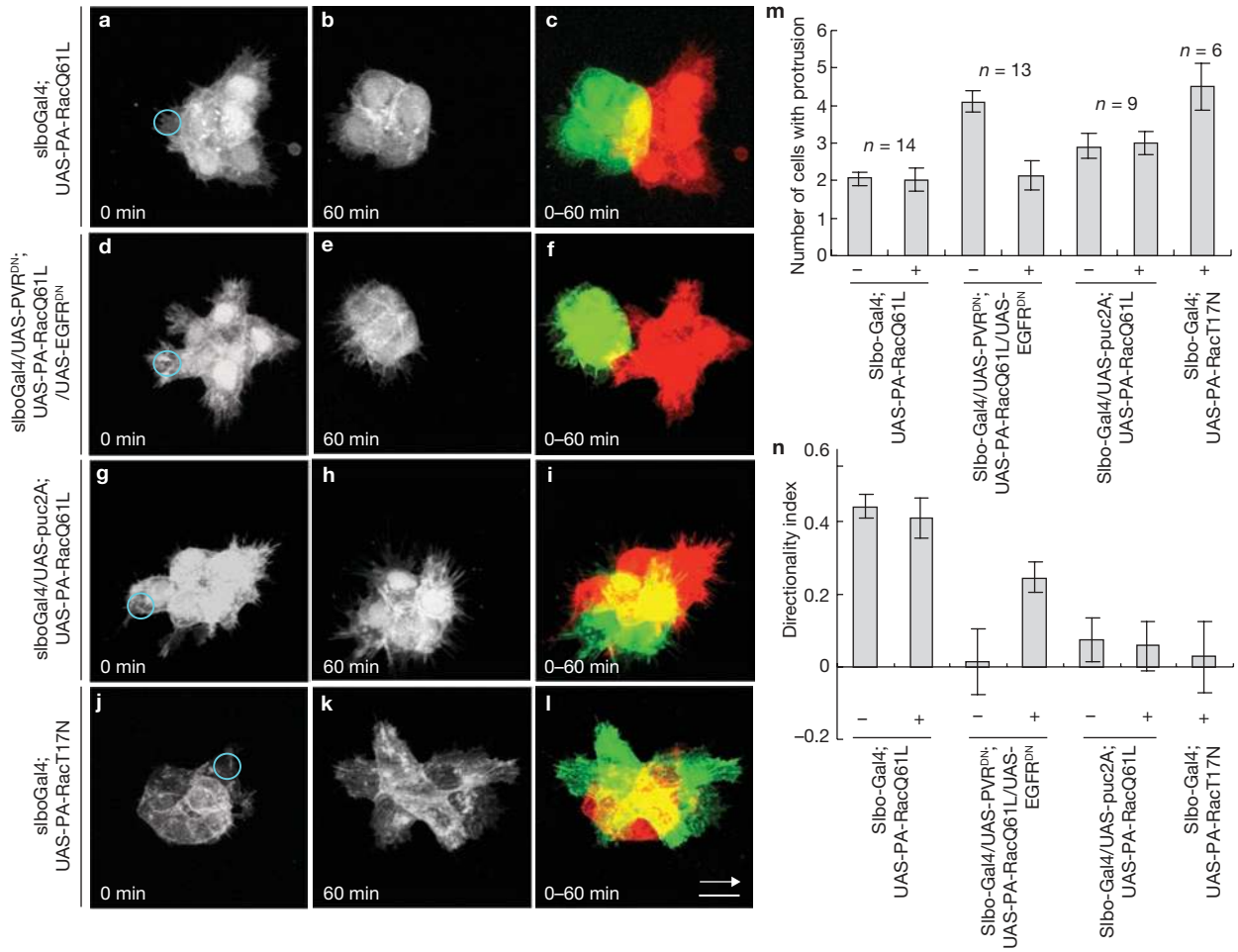

Figure 4 Local photoactivation or photoinactivation of Rac in one cell affects the morphology and behaviour of other cells in the group. (**a**–**l**) Confocal images of border cell clusters before (0 min) and after (60 min) photoactivation. Circles indicate areas of laser treatment. The white arrow in **l** indicates the direction the border cells would normally migrate and applies to all panels. Scale bar, 10 μm. In **c**, **f**, **i** and **l**, red shows the starting position and green shows the ending position. (**m**) The average number of cells sending protrusions simultaneously within one cluster was calculated from three-dimensional reconstructed images (see Methods and Supplementary Fig. 6). – and + indicate before and after photoactivation. (**n**) Directionality indices were calculated from the same samples (see Methods). Error bars show the s.d.

To quantify these results, we developed an automated method to count the number of protruding cells (Supplementary Information, Fig. S6) and calculated the directionality index, which measures the degree of polarization of the cell cluster[20]. PA-RacQ61L treatment rescued the PVR^{DN} and $EGFR^{DN}$ polarization defect and the number of protruding cells to nearly wild-type (Fig. 4m, n).

Inhibition of the Jun N-terminal kinase (JNK) pathway also reduces the directionality index[24] (Fig. 4n). The JNK pathway helps to coordinate border cell movement by promoting cohesion between border cells. To test the hypothesis that cluster cohesion is important for the non-autonomous effects of Rac, we monitored the effect of PA-RacQ61L in cells with reduced JNK signalling. Photoactivation of Rac at the back of clusters with impaired JNK signalling did not cause retraction of protrusions that were extended in other directions and resulted in little net movement of the cluster (Fig. 4g–i). The same effect was observed whether JNK signalling was reduced by expression of the JNK phosphatase Puckered (UAS-Puc2A) or by expressing a dominant-negative form of the kinase (not shown).

The inability of PA-RacQ61L to rescue the JNK knockdown phenotype could have been because JNK signalling is required autonomously downstream of Rac to generate lamellipodial protrusion. However, PA-RacQ61L induced autonomous cell protrusion in the direction of illumination, even in cells over-expressing Puc2A (Fig. 4g–i). Therefore, JNK signalling is not required downstream of Rac to promote protrusion, consistent with the published observation that reduction of JNK signalling does not lead to reduced protrusion[24]. Together, these results suggest that JNK signalling is required for the non-autonomous propagation of directional information from the cell with highest Rac activity to the other cells of the cluster. This could be due to direct mechanical coupling of the cells or through signalling pathways downstream of adhesion receptors or both.

Our results suggested that Rac is normally active in all the cells of the cluster, that the leading cell has a higher level of Rac activity, and that this asymmetry is lost in PVR^{DN}- and $EGFR^{DN}$-expressing cells. To test this we took advantage of a Rac fluorescence resonance energy transfer (FRET) biosensor[25]. When expressed in *Drosophila* S2 cells, biosensor activity increased in response to EGF stimulation, and the increase was blocked by co-expression of dominant-negative Rac (Supplementary Information, Fig. S7a–k). We generated transgenic flies expressing the biosensor under

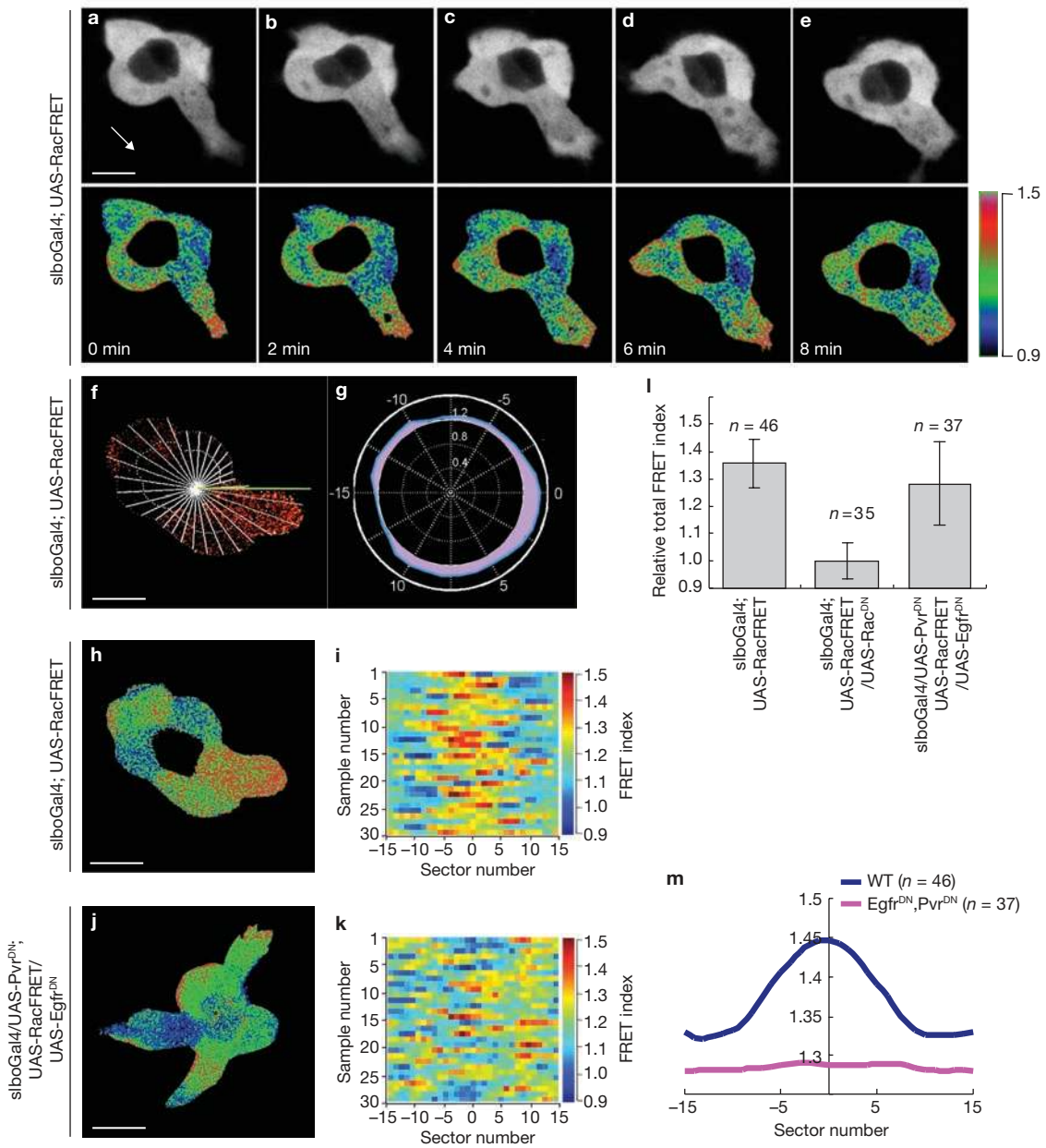

Figure 5 Rac activity pattern in migrating border cell clusters. (**a**–**e**) A time lapse series of migrating border cells. Top, yellow fluorescent protein (YFP) channel only; bottom, processed FRET signal. (**f**) FRET image of wild-type border cells displayed with Red-Hot pseudocolour divided into 30 sectors. The yellow line shows the direction of migration. The white circle indicates the central region that was excluded from the analysis. (**g**) Average FRET index from **f** plotted in a radar map. Index higher than 1.2 is highlighted in purple. (**h**, **j**) Representative FRET patterns in wild-type (**h**) and EGFR^{DN}- and PVR^{DN}-expressing (**j**) border cells. (**i**, **k**) Heatmaps from 30 examples of the genotypes shown in **h** and **j**, respectively. Each row represents the FRET signal distribution of an individual border cell cluster. Positions from –15 to 15 plotted on the *x*-axis correspond to the sectors, where 0 represents the front of the cluster. (**l**) FRET indices in border cells of the indicated genotypes. All results were normalized to the index of Rac^{DN}. (**m**) Distributions of average FRET indices in wild-type (blue) and PVR^{DN}/EGFR^{DN} border cells, plotted as a function of sector number, where 0 represents the front. Scale bars, 10 μm.

the control of Gal4/UAS. When expressed with *slbo*-Gal4, we consistently observed a FRET signal in border cells (Supplementary Information, Fig. S7l, m), and this was dramatically reduced upon co-expression of dominant-negative Rac (Supplementary Information, Fig. S7n, o). Moreover, the signal within the border cell cluster was asymmetric and seemed highest in elongating protrusions, which were most prominent in the leading cell (Fig. 5a–e). This FRET signal was inhibited by co-expression of RacT17N (Fig. 5l). To quantify the asymmetry we divided the border cell cluster into 30 sectors (where sector 0 represents the front of the cluster and –15 and +15 represent the rearmost sector) and measured the FRET index in each sector for more than 30 clusters (Fig. 5f–g). As predicted, the Rac activity was highest at the front (between sectors –5 and +5) and lowest at the back (Fig. 5h, i, m). We then measured the Rac activity in more than 30 border cell clusters expressing PVR^{DN} and EGFR^{DN} and found no difference between front and back (Fig. 5j, k, m), consistent with the proposal that asymmetric Rac activation requires guidance receptor input. In the absence of such asymmetry, non-directional signals activate Rac uniformly, stimulating random protrusion.

During normal morphogenesis and in tumour metastasis, many cells move in interconnected groups in a process termed collective cell migration[4–7]. Border cells represent one model for the study of such movements. We previously found that guidance receptor signalling not only promotes border cell protrusion at the front of the cluster but also polarizes the group so as to inhibit protrusion at the rear[20]. However, it was unclear to what extent each cell sensed direction independently or whether they did so collectively and what intracellular signal(s) downstream of the receptors would be sufficient to polarize the group[26]. The results presented here demonstrate that a local increase in Rac activity is sufficient not only to stimulate protrusion autonomously in the treated cell but also to cause retraction of side and back cells, resulting in net cluster polarization and movement in the direction of highest Rac activity. Conversely, inhibition of Rac in the lead cell caused the other cells to protrude in all directions, as if guidance receptor activity were lost. These results suggest that elevated guidance activity at the front of the cluster activates Rac to a higher level in the front cell and that this is sufficient to set the direction of migration for the whole group. Despite the fact that receptor tyrosine kinases activate many downstream signalling pathways, other pathways do not appear to be necessary, although they may have redundant or overlapping roles. Thus, asymmetric Rac activity is key for direction sensing *in vivo*. We also show that JNK signalling is required to transmit the guidance signal between cells of the cluster. This work further suggests that photoactivatable proteins are likely to be a powerful new class of tools for the manipulation of protein activities with fine spatial and temporal control to address a variety of biological questions in animals. □

METHODS

Methods and any associated references are available in the online version of the paper at http://www.nature.com/naturecellbiology/

Note: Supplementary information is available on the Nature Cell Biology website.

ACKNOWLEDGEMENTS

This work was supported by grants GM046425 to D.J.M. and GM 057464 to K.M.H. and by the Cell Migration Consortium.

AUTHOR CONTRIBUTIONS

X.W. carried out the experiments documented in Figs 1–3 and Supplementary Information, Figs S1–S5. L.H. carried out the experiments shown in Figs 4–5 and Supplementary Information, Figs S5–S7. X.W. made all of the transgenic flies and helped L.H. to collect FRET data in Fig. 5. Y.W. developed and provided the PA-Rac constructs and advised X.W. on their use. K.M.H. and D.J.M. coordinated the study. D.J.M. prepared the final version of the manuscript, based on contributions from all authors.

COMPETING FINANCIAL INTERESTS

The authors declare no competing financial interests.

Published online at http://www.nature.com/naturecellbiology/
Reprints and permissions information is available online at http://npg.nature.com/reprintsandpermissions/

1. Ridley, A. J., Paterson, H. F., Johnston, C. L., Diekmann, D. & Hall, A. The small GTP-binding protein Rac regulates growth factor-induced membrane ruffling. *Cell* **70**, 401–410 (1992).
2. Sander, E. E. & Collard, J. G. Rho-like GTPases: their role in epithelial cell-cell adhesion and invasion. *Eur. J. Cancer* **35**, 1302–1308 (1999).
3. Fukata, M. & Kaibuchi, K. Rho-family GTPases in cadherin-mediated cell-cell adhesion. *Nature Rev. Mol. Cell Biol.* **2**, 887–897 (2001).
4. Friedl, P. & Gilmour, D. Collective cell migration in morphogenesis, regeneration and cancer. *Nature Rev. Mol. Cell Biol.* **10**, 445–457 (2009).
5. Weijer, C. J. Collective cell migration in development. *J. Cell Sci.* **122**, 3215–3223 (2009).
6. Rorth, P. Collective cell migration. *Annu. Rev. Cell Dev. Biol.* **25**, 407–429 (2009).
7. Bidard, F. C., Pierga, J. Y., Vincent-Salomon, A. & Poupon, M. F. A "class action" against the microenvironment: do cancer cells cooperate in metastasis? *Cancer Metastasis Rev.* **27**, 5–10 (2008).
8. Wu, Y. I. *et al.* A genetically encoded photoactivatable Rac controls the motility of living cells. *Nature* **461**, 104–108 (2009).
9. Silver, D. L. & Montell, D. J. Paracrine signaling through the JAK/STAT pathway activates invasive behavior of ovarian epithelial cells in *Drosophila*. *Cell* **107**, 831–841 (2001).
10. Silver, D. L., Geisbrecht, E. R. & Montell, D. J. Requirement for JAK/STAT signaling throughout border cell migration in *Drosophila*. *Development* **132**, 3483–3492 (2005).
11. Bai, J., Uehara, Y. & Montell, D. J. Regulation of invasive cell behavior by Taiman, a *Drosophila* protein related to AIB1, a steroid receptor coactivator amplified in breast cancer. *Cell* **103**, 1047–1058 (2000).
12. Duchek, P. & Rorth, P. Guidance of cell migration by EGF receptor signaling during *Drosophila* oogenesis. *Science* **291**, 131–133 (2001).
13. Duchek, P., Somogyi, K., Jekely, G., Beccari, S. & Rorth, P. Guidance of cell migration by the *Drosophila* PDGF/VEGF receptor. *Cell* **107**, 17–26 (2001).
14. McDonald, J. A., Pinheiro, E. M., Kadlec, L., Schupbach, T. & Montell, D. J. Multiple EGFR ligands participate in guiding migrating border cells. *Dev. Biol.* **296**, 94–103 (2006).
15. McDonald, J. A., Pinheiro, E. M. & Montell, D. J. PVF1, a PDGF/VEGF homolog, is sufficient to guide border cells and interacts genetically with Taiman. *Development* **130**, 3469–3478 (2003).
16. Wang, X., Adam, J. C. & Montell, D. Spatially localized Kuzbanian required for specific activation of Notch during border cell migration. *Dev. Biol.* **301**, 532–540 (2007).
17. Murphy, A. M. & Montell, D. J. Cell type-specific roles for Cdc42, Rac, and RhoL in *Drosophila* oogenesis. *J. Cell Biol.* **133**, 617–630 (1996).
18. Geisbrecht, E. R. & Montell, D. J. A role for *Drosophila* IAP1-mediated caspase inhibition in Rac-dependent cell migration. *Cell* **118**, 111–125 (2004).
19. Prasad, M., Jang, A. C. C., Starz-Gaiano, M., Melani, M., & Montell, D. A. A protocol for culturing *Drosophila melanogaster* stage 9 egg chambers for live imaging *Nat. Protoc.* **2**, 2467–2473 (2007).
20. Prasad, M. & Montell, D. J. Cellular and molecular mechanisms of border cell migration analyzed using time-lapse live-cell imaging. *Dev. Cell* **12**, 997–1005 (2007).
21. Montell, D. J. Border-cell migration: the race is on. *Nature Rev. Mol. Cell Biol.* **4**, 13–24 (2003).
22. Jang, A. C., Chang, Y. C., Bai, J. & Montell, D. Border-cell migration requires integration of spatial and temporal signals by the BTB protein Abrupt. *Nature Cell Biol.* **11**, 569–579 (2009).
23. Montell, D. J., Rorth, P. & Spradling, A. C. slow border cells, a locus required for a developmentally regulated cell migration during oogenesis, encodes *Drosophila* C/EBP. *Cell* **71**, 51–62 (1992).
24. Llense, F. & Martin-Blanco, E. JNK signaling controls border cell cluster integrity and collective cell migration. *Curr. Biol.* **18**, 538–544 (2008).
25. Kardash, E. *et al.* A role for Rho GTPases and cell-cell adhesion in single-cell motility in vivo. *Nat. Cell Biol.* **12**, 47–53 (2010).
26. Rorth, P. Collective guidance of collective cell migration. *Trends Cell Biol.* **17**, 575–579 (2007).

METHODS

***Drosophila* strains.** New transgenic fly lines were generated by Bestgene Inc. Amino-terminal-cherry tagged PA-RacQ61L, PA-RacT17N, the light insensitive control C450M-PA-RacQ61L (ref. 8) and the Rac FRET probe were inserted into the pUASt *Drosophila* expression vector using the Gateway recombination system (Invitrogen). P[slbo-GAL4] (ref. 27) drives UAS transgene expression in outer, migratory border cells, but not polar cells even though the endogenous *slbo* gene and protein product are expressed in both cell types[23]. P[UAS-MCD8-GFP] (ref. 28), P[UAS-moesin-GFP] (ref. 29), P[UAS-DRacT17N] and P[UAS-DRacV12] (ref. 30) have been described previously. P[UAS-PVR^{DN}] and P[UAS-EGFR^{DN}] were obtained from P. Rørth[13]. P[UAS-Puc2A] and P[UAS-DnBsk] were obtained from E. Martin-Blanco[24]. All stocks were maintained at room temperature. Before dissection, flies were maintained at 29 °C overnight to increase transgene expression levels. This incubation had no negative effect on border cell migration.

Imaging and photomanipulation. *Drosophila* egg chambers were dissected and mounted in Schneider's insect medium supplemented with 20% fetal bovine serum (FBS) and 0.10 mg/ml insulin as described[19,20]. Photoactivation, time-lapse imaging and three-dimensional (3D) morphological reconstruction were carried out using a Zeiss 510-Meta confocal microscope using a 63X, 1.4 numerical aperture lens with 2X zoom. To photoactivate, the 458 nm laser was set at 10% power for 0.1 ms per pixel in a 7 μm spot and the photoactivation scan took ~25 s. After 30 s, border cells were imaged using 568 nm. This series of steps was repeated for the duration of the time-lapse experiment. Where indicated, 15–20 *z* planes separated by 1.5 μm were obtained before and after photoactivation (samples were illuminated every 80 s for 1 h). 3D reconstructions were rendered using Imaris software. S2 cells were transfected with the Rac FRET vector with or without the Rac^{DN} vector using the QIAGEN Effectine Kit. Cells were transferred to serum-free medium 48 h after transfection and cultured for another 6 h. Then the cells were transferred into 4-well Lab-Tek chamber slides for 1 h before imaging. A final concentration of 150 ng/ml EGF was added to induce Rac activity. Rac FRET probe was kindly provided by Erez Raz. FRET experiments in S2 cells were carried out on an Olympus IX81 microscope using a 40X, 1.3 numerical aperture oil immersion objective. Cyan (CFP) and yellow fluorescent protein (YFP) signals were recorded using Chroma 86002BS dichroic mirror sets: CFP (excitation, 436/10 nm; emission, 470/30 nm (transmission wavelength/band width), YFP (excitation, 436/10 nm; emission, 535/30 nm). A 25% neutral density filter was used to reduce bleaching.

FRET images of live cultured egg chambers were acquired with Zeiss LSM710 microscope. A 458 nm laser was used to excite the sample. CFP and YFP emission signals were collected through channel I (470–510 nm) and channel II (525–600 nm) respectively. To capture single, high-resolution, stationary images, a 40X/1.1 water immersion objective was used. CFP and YFP images were acquired simultaneously for most of the experiments. Sequential acquisition of CFP and YFP channels in alternative orders were tested and gave the same result as simultaneous acquisition. CFP and YFP images were first processed by ImageJ software. A background region of interest was subtracted from the original image. The YFP images were registered to CFP images using the TurboReg plugin. Gaussian smooth filter was then applied to both channels. The YFP image was thresholded and converted to a binary mask with background set to zero. The final ratio image was generated with the MATLAB program, during which only the unmasked pixel was calculated and all YFP/CFP ratios (FRET index) were adjusted to the initial FRET ratio to reduce the effect of bleaching. FRET images were analysed using MATLAB. The border cell cluster was first isolated with its centre calculated based on its contour. Then the cluster was divided into 30 sectors, each of which occupies a 12-degree central angle. Because the centre of the cluster contains the polar cells, which do not express slbo-Gal4 and therefore were devoid of signal, only the signal within the distal third of each sector from the centre was calculated. The average signal of each sector become a vector of length 31. The first and last element corresponding to the –15 and 15 sectors were the same, so the front of border cell was centred at zero. A heatmap was composed using 30 vectors from different egg chambers with the same genotype. All vectors for each genotype were further averaged and smoothed to generate a representative curve of the FRET distribution around the cluster.

Measurement of migration speed, protrusion number, directionality index and protrusion density. The distance of the centre of the border cell cluster between the first and last time points in a time lapse series was measured with Imaris software. This distance divided by the elapsed time gave the speed. Cell protrusions were counted as follows: a circle corresponding to the average cluster diameter was drawn and any extension more than 2 μm beyond that was considered a protrusion. The directionality index (DI) was calculated using the following equation: $DI = (\sum_{i=1}^{N} \vec{P}_i \bullet \vec{d}\,) / \sum_{i=1}^{N} \left\| \vec{P}_i \right\|$

where N is the total number of major protrusions, $\vec{P}_i$ is the ith protrusion vector, and $\vec{d}$ is the unit vector of migration direction. The protrusion vector was calculated by fitting the major protrusion by a parabola whose peak together with the cluster centre gives the vector's direction and length. Protrusion density was generated by dividing the number of all the recognizable membrane protrusions by the estimated cell perimeter in μm. The morphology analysis and quantification were done in MATLAB.

Immunohistochemistry. *Drosophila* ovaries were dissected and fixed as described previously[31] and incubated with 1.4 units Alexa 488-conjugated phalloidin (Molecular Probes) per ml and 1 μg/ml 4,6-diamidino-2-phenylindole (DAPI) before imaging on a Zeiss 510-Meta confocal microscope and 3D reconstruction using Imaris software.

27. Rorth, P. *et al.* Systematic gain-of-function genetics in *Drosophila*. *Development* **125,** 1049–1057 (1998).
28. Lee, T. & Luo, L. Mosaic analysis with a repressible cell marker for studies of gene function in neuronal morphogenesis. *Neuron* **22**, 451–461 (1999).
29. Edwards, K. A., Demsky, M., Montague, R. A., Weymouth, N. & Kiehart, D. P. GFP-moesin illuminates actin cytoskeleton dynamics in living tissue and demonstrates cell shape changes during morphogenesis in *Drosophila*. *Dev. Biol.* **191**, 103–117 (1997).
30. Luo, L., Liao, Y. J., Jan, L. Y. & Jan, Y. N. Distinct morphogenetic functions of similar small GTPases: *Drosophila* Drac1 is involved in axonal outgrowth and myoblast fusion. *Genes Dev.* **8**, 1787–1802 (1994).
31. McDonald, J. A. & Montell, D. J. Analysis of cell migration using *Drosophila* as a model system. *Methods Mol. Biol.* **294**, 175–202 (2005).

nature cell biology

DOI: 10.1038/ncb2061

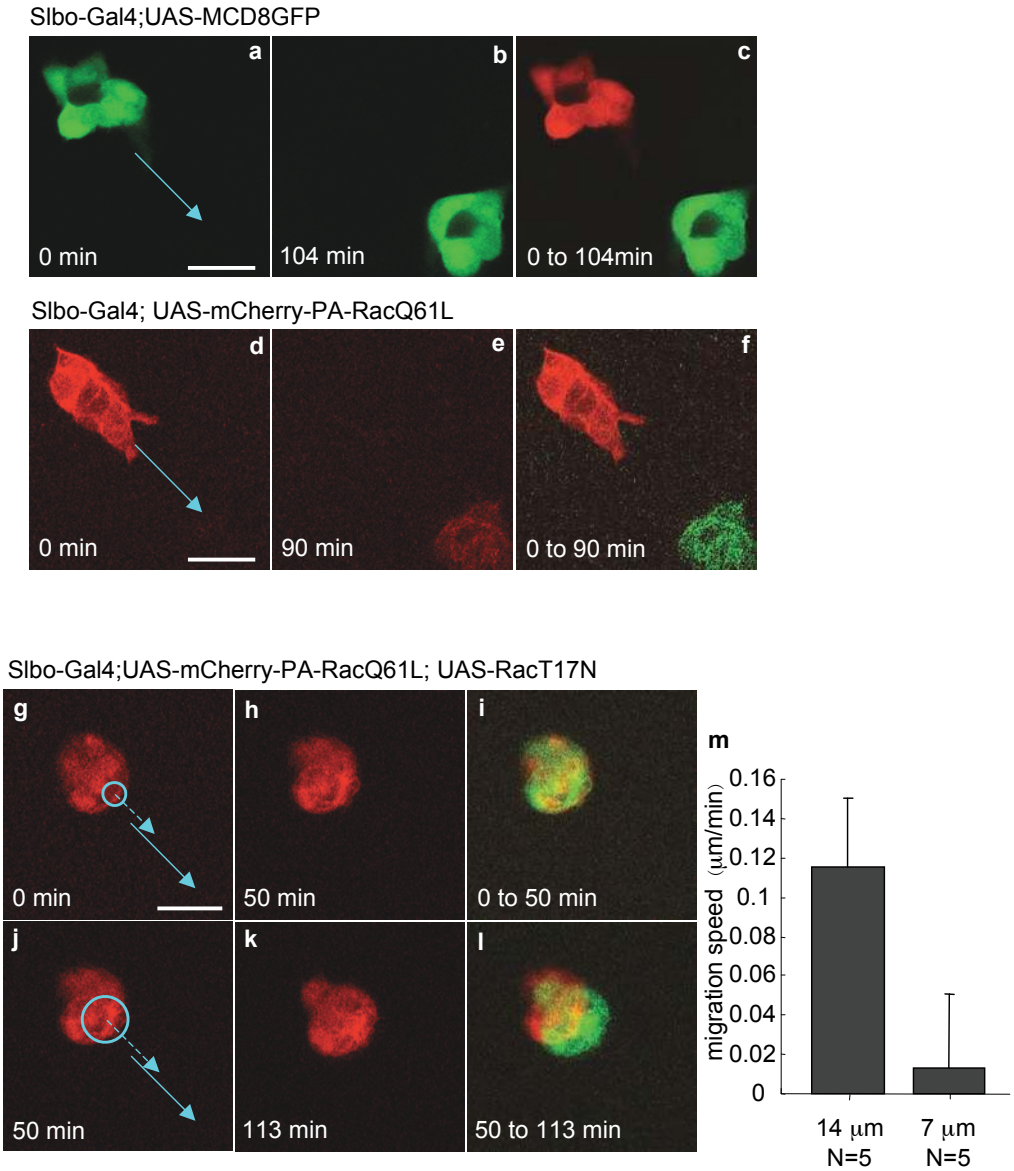

Figure S1 Normal border cell migration in the absence of a light stimulus and effect of PA-RacQ61L in border cells expressing dominant-negative Rac. Still images from timelapse movies of border cells of the indicated genotypes without light treatment. The blue arrow shows the normal direction of movement, which is unperturbed by expression of PA-RacQ61L in the absence of illumination. The images in **c** and **f** represent the superimposition of the images shown in panels **a**, **b** and **d, e,** respectively, with the starting position shown in red and the ending position shown in green. **g-i**) Border cell clusters expressing PA-RacQ61L and dominant-negative Rac (RacT17N) under the control of *slbo*-Gal4. **g-l**) Illumination of a portion of one cell using a 7μm diameter laser did not result in forward movement. **j-i**) Illumination of approximately half of the cluster using a 14μm diameter beam did result in slow forward movement. In **g** and **j** solid arrows indicate the normal direction of migration; circles indicate where the laser light was applied once/minute. Dashed arrows indicate the direction the cells would move in response to the light. Panel **i** shows the superimposition of the iamges shown in **g** and **h** with the starting position shown in red and the ending position shown in green. Similarly panel **l** shows the superimposition of the images in **j** and **k**. **m**) Average migration speeds for clusters in response to illumination with the indicated size light beams. Values represent the average of five independent experiments and error bars represent the standard deviation. Scale bars, 20 μm.

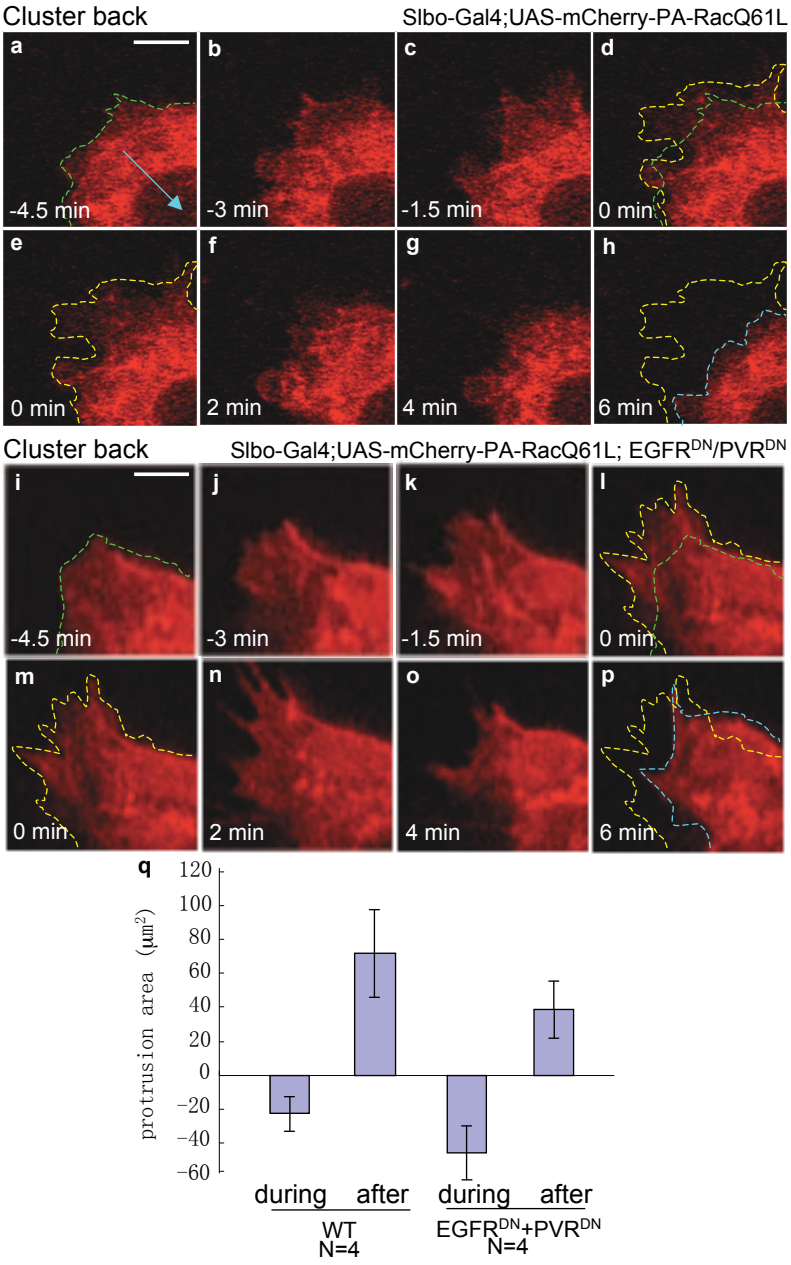

Figure S2 Rapid responses of border cells to photoactivation of Rac and cessation of the stimulus. The rear edges of wild-type (**a-d** and **e-h**) or PVR^{DN}- and $EGFR^{DN}$-expressing (**i-l** and **m-p**) border cell clusters are shown. Samples were illuminated at the rear once every 90 seconds for 4.5 minutes. Light treatment was stopped at time 0 and the response monitored for an additional 6 minutes. The dashed green lines show the contour of the cell edge at the beginning of the experiment. The yellow lines show the edge when the light stimulation was stopped and the blue lines trace the contour at the end of the experiment. **q**)Average protrusion area changes during photoactivation and after cessation of the light stimulus in both WT and PVR^{DN}- and $EGFR^{DN}$-expressing border cells. Negative numbers indicate rearward protrusion and positive numbers represent rear retraction. Values represent the average of the indicated number (N) of experiments and error bars show the standard deviation. Scale bars, 5 μm.

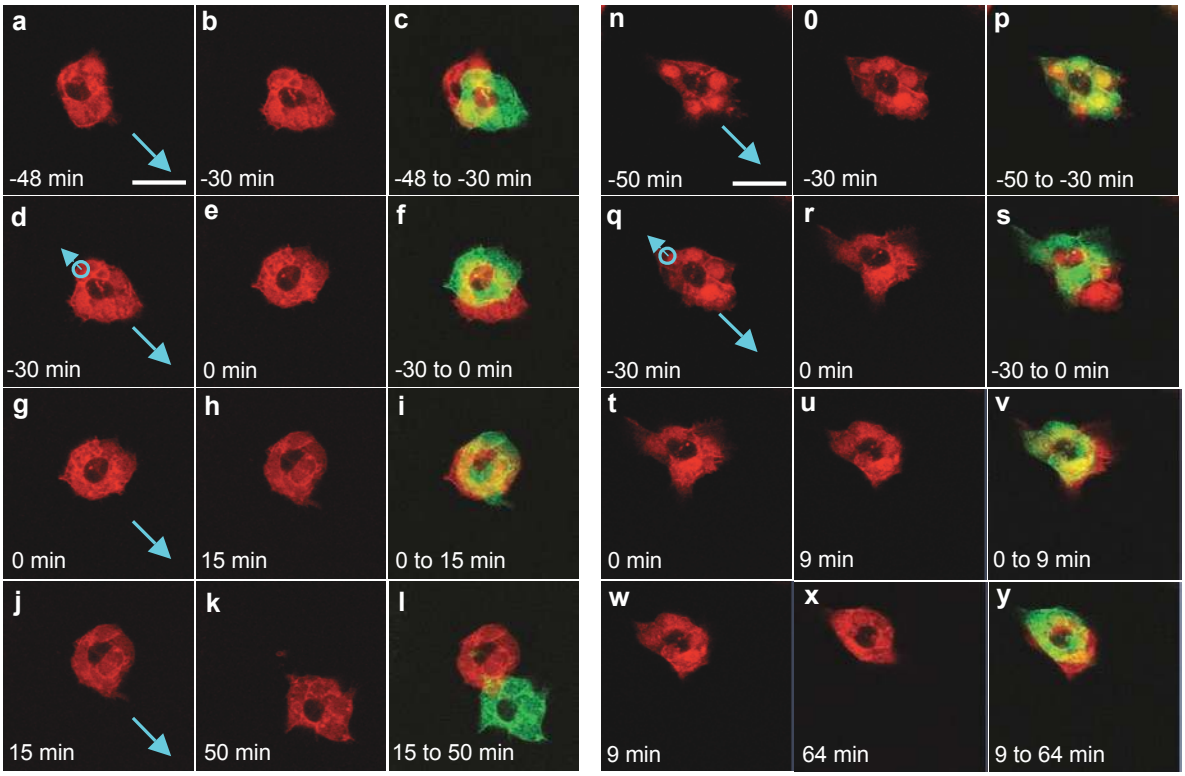

Slbo-Gal4;UAS-mCherry-PA-RacQ61L

Slbo-Gal4;UAS-mCherry-PA-RacQ61L; EGFR^{DN}/PVR^{DN}

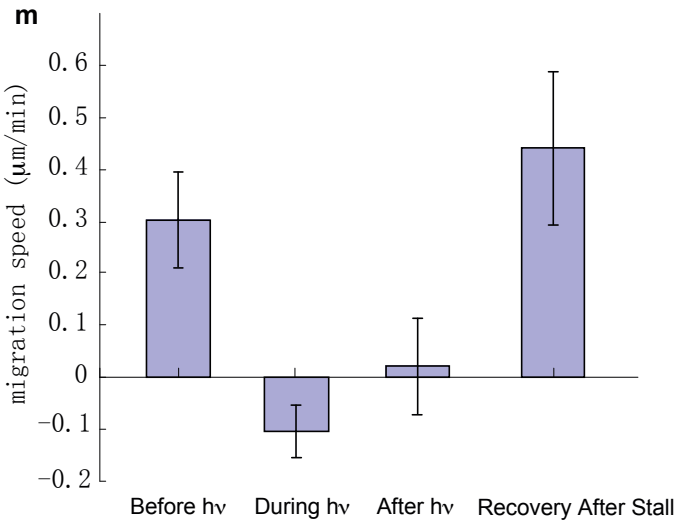

Lag time is from 9 to 48 mins in 7 independent experiment
Average lag time: 24+/-12 mins

Figure S3 Recovery of forward migration after cessation of rear illumination. (**a-c**) Before illumination, wild-type border cells expressing PA-RacQ61L migrate in the normal forward direction (solid arrow). (**d-f**) Photoactivation at the rear drives reverse border cell migration in the indicated time period. (**g-i**) When photoactivation is stopped (t=0), border cells stall for a variable period of time before regaining forward migration (**j-l**). Panel **c** shows the superimposition of the images in **a** and **b** with the starting position shown in red and the ending position shown in green. Similarly panel **f** shows the superimposition of the images in **d** and **e**, etc. (**m**) Comparison of average migration speeds before any treatment (before), during rear photoactivation of RacQ61L (during), immediately after cessation of the light stimulus (after) and then once forward migration resumed (recovery after stall). Values represent the average of seven experiments. Error bars show the standard deviation. The stall time ranged from 9-48 minutes and averaged 24+/-12 minutes). (**n-p**) Prior to illumination, border cells expressing PVR^{DN} and EGFR^{DN} fail to move forward, unlike wild-type. (**q-s**) Photoactivation at the rear (circle) drives rearward movement (arrow) over the indicated time period. (**t-y**) Upon cessation of the light at t=0, the cluster stops. Scale bars, 20 μm.

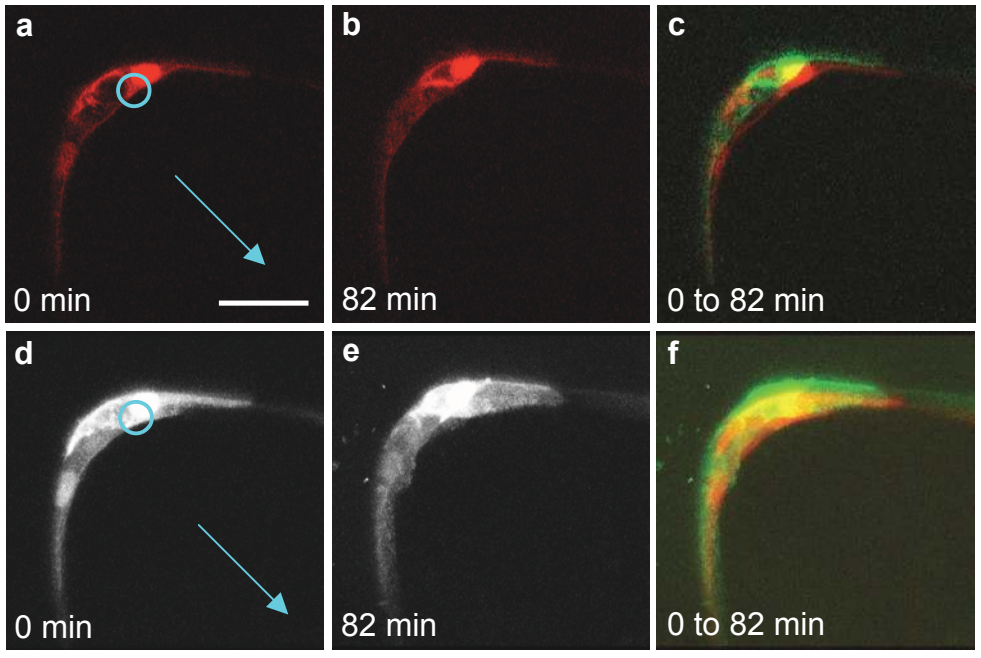

Figure S4 Effect of PA-RacQ61L in border cells lacking STAT or SLBO. 2D images (**a-c and g-i**) and 3D reconstructions (**d-f, and j-l**) of border cell clusters expressing UAS-domeΔCYT, a dominant-negative form of the receptor for the JAK/STAT pathway (**a-f**) or mutant for *slbo* (**g-l**). In the panels with two colors, red shows the starting position and green shows the ending position. For both genotypes, at least 5 independent experiments were carried out and all of them showed the same phenotype. The blue arrow shows the normal direction of border cell movement; circles indicate where the laser light was applied once every minute. The slight apparent displacement is due to growth of the egg chamber rather than movement of any cell. Scale bars, 20 μm.

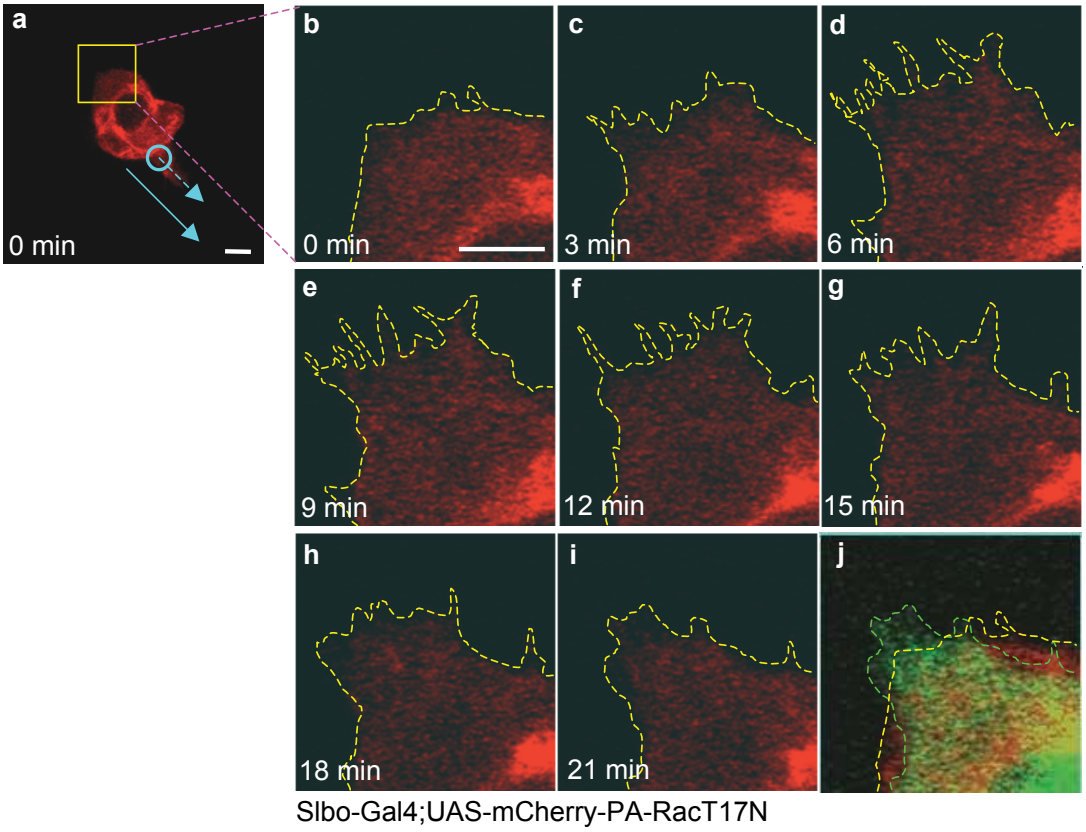

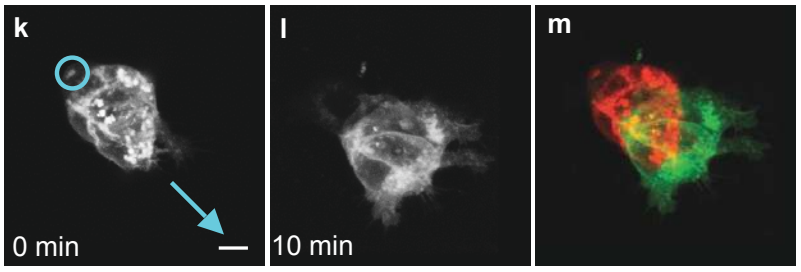

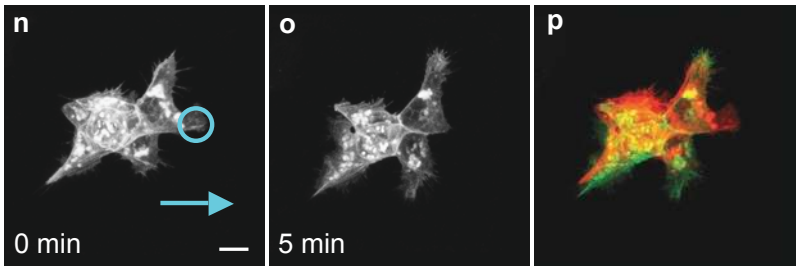

Figure S5 Effects of local inactivation of Rac. Confocal micrographs of cells expressing photoinactivatable Rac (PA-RacT17N) (**a-j**) Images from a timelapse series showing morphological change at the back of an otherwise wild-type border cell cluster in response to photo-inactivation of Rac in the forward-directed protrusion of the leading cell. The arrow shows the normal direction of migration; the circle indicates the position of laser illumination. Dashed yellow lines outline the contour of the cluster rear, which is shown at high magnification in panels b-j. Panel **j** shows the superimposition of panels **b** and **i**, with the starting contour in yellow and the ending contour in green. (**k-m**) In otherwise wild-type cells, inactivation of Rac at the rear of the border cell cluster promoted protrusion at the front. Panel **m** shows the superimposition of the images in **k** (red) and **l** (green). (**n-p**) In Pvr^{DN} and Egfr^{DN}-expressing cells, inactivation of Rac at the front caused local retraction. Panel **p** shows the overlay of the images in **n** (red) and **o** (green). The arrows indicate the normal direction of border cell migration. The circles indicate the illuminated regions. Scale bar, 5 um.

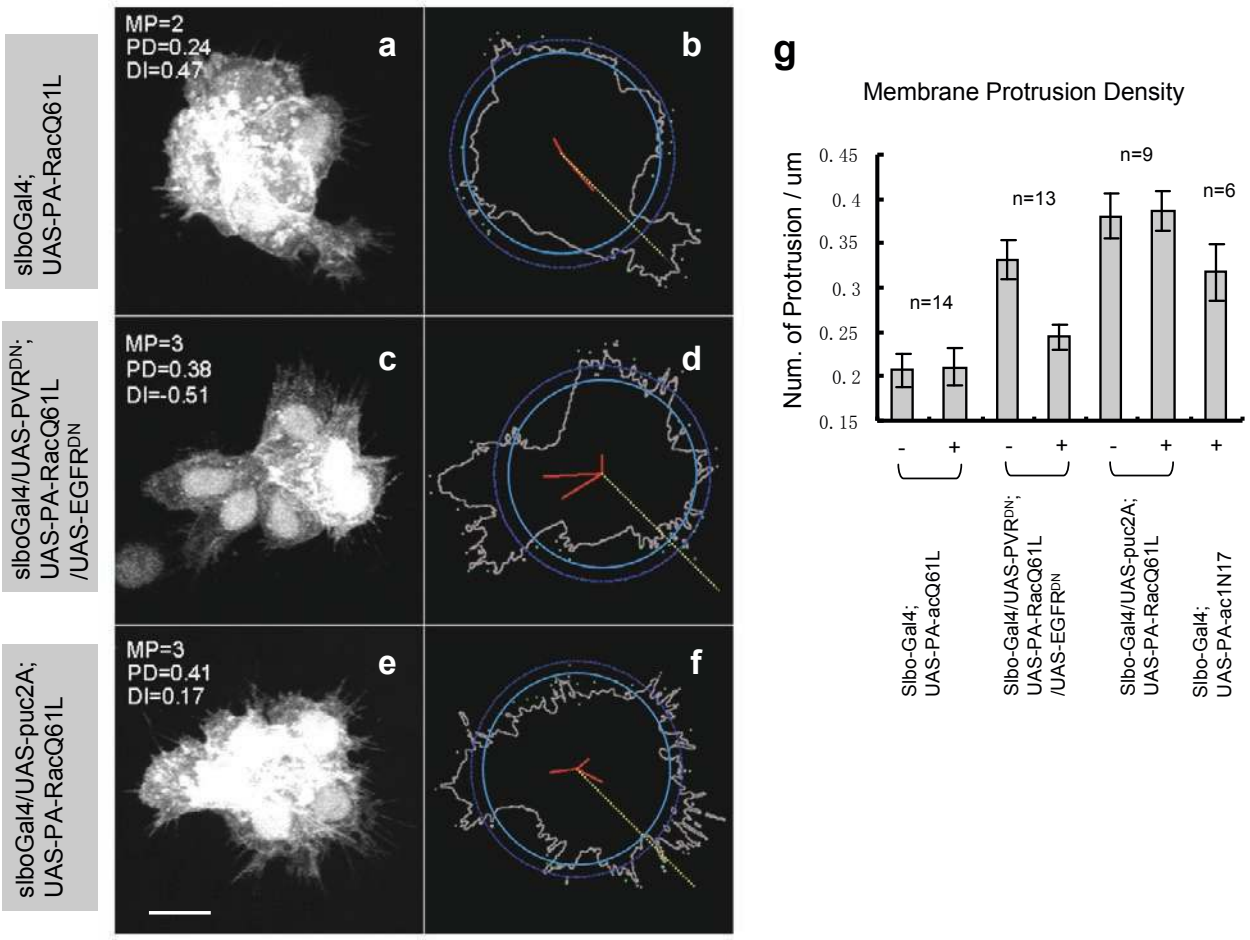

Figure S6 Rescue of PVR^{DN} and EGFR^{DN} , but not JNK deficiency, by PA-RacQ61L. Representative original (**a, c, e**) and processed (**b, d, f**) images of border cell clusters of the indicated genotypes. The blue circle shows the average cluster radius. Scale bar is 10um. Major protrusions (MP) were defined as extensions at least 2μm beyond the average cluster radius and broader than 2μm, were identified automatically using MatLab; protrusion density (PD), was calculated by dividing the number of all the recognizable membrane protrusions by the estimated cell perimeter in μm; directionality index (DI) indicates the fraction of forward-directed protrusions relative to the total number of protrusions. In b, d, and f, the cluster contour is shown in gray; the inner cyan circle shows the average cell perimeter; the outer blue circle shows the threshold for major protrusion detection; each recognized protrusion is labeled by a green dot; the migration direction is indicated by yellow line; red vectors represent major protrusions and the length of the each vector is proportional to the length of protrusion it represents. (**g**) Histogram showing protrusion density for the indicated genotypes. Values represent the average of the indicated number (N) of experiments and error bars show the standard deviation.

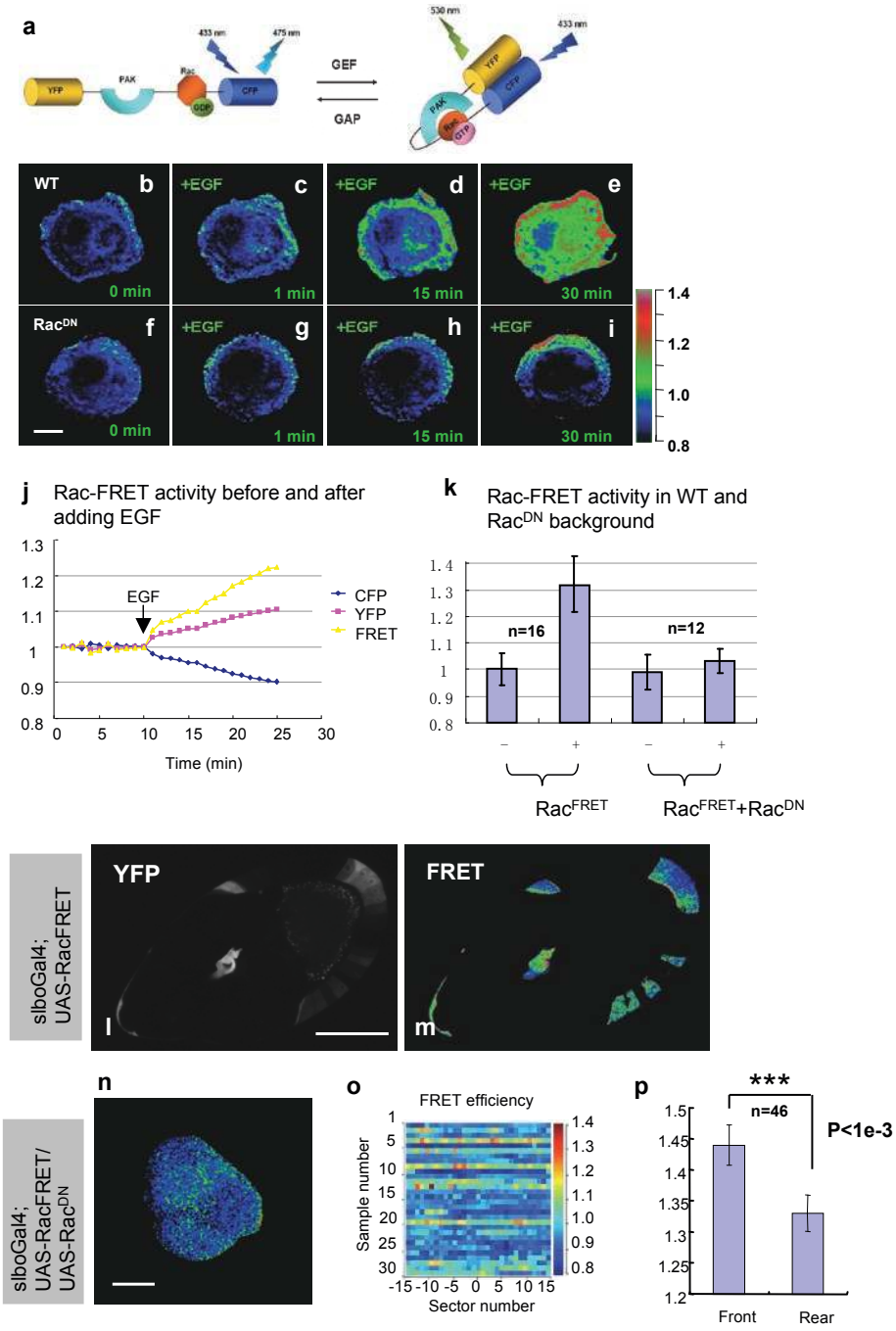

Figure S7 Detection of Rac activation in Drosophila cells using a FRET probe. (**a**) Schematic of the Rac FRET probe adpated from[24] before and after activation. (**b-i**) YFP/CFP ratio in S2 cells in response to EGF stimulation, with or without co-expression of RacT17N (Rac^{DN}). A time series of ratio FRET images is shown. Scale bar is 10um. (**j**) Quantiative changes in CFP and YFP fluorescence and Rac FRET efficiency before and after addition of EGF. Each channel was normalized to its intensity prior to EGF treatment. (**k**) Average Rac FRET efficiencies before (-) and 30 min after (+) addition of EGF. Values represent the average of the indicated number (N) of experiments and error bars show the standard deviation. (**l**) YFP expression from the Rac FRET probe expressed with *slbo*-Gal4 in a stage 9 egg chambers. Scale bar is 50um. (**m**) Rac FRET pattern was processed in the same stage 9 egg chamber. (**n**) Rac FRET pattern in border cells expressing dominant-negative Rac. Scale bar is 10um. (**o**) Heatmap showing relative FRET efficiency in 30 sectors for 30 border cell clusters co-expressing the FRET probe and dominant-negative Rac. Compare to wild-type which is shown in Figure 5l. (**p**) In WT border cells, the mean relative FRET efficiencies at the front (sectors -3 to 3) and the rear (sectors -12 to -15 and 12 to 15) were calculated. P-value was given by two sided t-test. Values represent the average of the indicated number (N) of experiments and error bars show the standard deviation.